CEA Comité Español de Automática
XLVII JORNADAS DE AUTOMÁTICA CÓRDOBA 2026
UNIVERSIDADE DA CORUÑA

Jornadas de Automática

Asymmetric Reset Control for Shape Memory Alloy Actuators

Carmen Ballester[a,*], Víctor Muñoz[a], Dorin Copaci[a], Luis Moreno[a], Dolores Blanco[a]

[a] *Universidad Carlos III de Madrid, Avda. Universidad 30, 28911 Leganés, España*

To cite this article: Ballester, C., Muñoz, V., Copaci, D., Moreno, L., Blanco, D. 2026. Asymmetric Reset Control for Shape Memory Alloy Actuators. Jornadas de Automática, 47. https://doi.org/10.17979/ja-cea.2026.47.13727

Resumen

Los actuadores de Shape Memory Alloy (SMA) son una alternativa a los motores convencionales en robótica por su elevada relación fuerza-peso, tamaño compacto y funcionamiento silencioso. Sin embargo, su funcionamiento térmico plantea retos de control. La activación puede controlarse mediante calentamiento eléctrico, pero la recuperación depende del enfriamiento pasivo. Esto genera un comportamiento asimétrico que limita la frecuencia de operación y degrada el seguimiento de trayectorias cíclicas. Los enfoques actuales abordan principalmente no linealidades como histéresis e incertidumbre paramétrica, mientras que los errores acumulados durante la recuperación reciben menor atención.

Este trabajo propone una estrategia asimétrica de reset control para mitigar la acumulación integral asociada a la recuperación del actuador. Se introducen acciones de reset parcial sobre el término integral de un PID. La dinámica en bucle cerrado se deriva mediante un modelo fenomenológico y se analiza mediante Lyapunov. La validación experimental demuestra una mejora del seguimiento durante calentamiento y una menor demanda de control, manteniendo un rendimiento global comparable.

Palabras clave: Sistemas de control de movimiento, Estructuras Inteligentes, Estabilidad de sistemas híbridos, Sistemas mecatr ónicos

Estrategia Asimétrica de Reset Control para Aleaciones con Memoria de Forma

Abstract

Shape-memory alloy (SMA) actuators are an alternative to conventional motors in robotics due to their high force-to-weight ratio, compact size, and silent operation. However, their thermal operating principle poses control challenges. Activation can be controlled by electrical heating, but recovery depends on passive cooling. This generates asymmetric behavior that limits the operating frequency and degrades tracking in repetitive motions. Current approaches mainly address nonlinearities such as hysteresis and parametric uncertainty, while errors accumulated during recovery have received less attention.

This work proposes an asymmetric reset control strategy to mitigate the integral accumulation associated with the thermal recovery of SMAs. Partial reset actions are introduced on the integral term of a PID. The closed-loop dynamics are derived using a phenomenological model and analyzed via Lyapunov criteria. Experimental validation demonstrates improved tracking during heating and reduced cumulative control demand, while maintaining comparable overall performance.

Keywords:
Motion Control Systems, Smart Structures, Stability of hybrid systems, Mechatronic Systems

1. Introduction

Smart materials are defined as materials capable of modifying their physical properties in response to external stimuli such as temperature, electric fields, magnetic fields, or mechanical stress. Shape Memory Alloys (SMAs) are smart materials capable of producing recoverable deformations through thermally induced phase transformations. Their high force-to-weight ratio, compactness, silent operation, and lightweight

* Autor para correspondencia: cballest@ing.uc3m.es

characteristics have enhanced their use in different actuation applications, including soft robotics, biomedical devices, aerospace morphing structures, and bioinspired robotic systems (Copaci et al. (2020), Costanza and Tata (2020)).

One of the main challenges associated with SMA actuators is their limited actuation frequency, which arises from their thermally driven operating principle (Utter (2019)). Heating can be actively controlled to produce rapid contraction in one direction, whereas recovery in the opposite direction depends on cooling dynamics that cannot be directly actuated. This introduces an intrinsic asymmetry in actuator behavior: SMA actuators can generate fast activation movements but require considerably longer recovery times before subsequent actuation cycles.

Because of this actuation asymmetry, tracking errors accumulated during cooling may propagate into subsequent activation cycles, deteriorating closed-loop performance. This phenomenon becomes particularly relevant during repetitive motions and higher operating frequencies, where thermal recovery limitations introduce persistent tracking deviations. Additionally, SMA actuators present important control challenges derived from their intrinsic nonlinear behavior, including hysteresis, temperature dependence, phase transition dynamics, and thermomechanical coupling effects.

Among the different SMA actuator applications, conventional PID controllers remain widely employed due to their simplicity and ease of implementation (Jadhav et al. (2025)). However, different approaches have been proposed to address SMA nonlinearities and improve control performance. Model-based compensation techniques have employed hysteresis representations such as Müller-Achenbach-Seelecke (Mandolino et al. (2023)) and Prandtl–Ishlinskii formulations (Al Janaideh et al. (2023)), while adaptive (Shi et al. (2024)) and robust control (Patterson et al. (2022)) strategies have also been explored to compensate parameter uncertainties and nonlinear effects.

Reset control systems provide an alternative framework to overcome some limitations of conventional linear controllers by introducing state discontinuities under predefined operating conditions Banos and Barreiro (2012). These controllers are especially suitable for mechatronic systems exhibiting memory effects and integral accumulation phenomena (Zhang and HosseinNia (2025), Karbasizadeh and HosseinNia (2022)), such as thermally driven SMA actuators. By selectively modifying controller states, reset mechanisms have demonstrated improved transient response and reduced accumulated error while preserving continuous-time closed-loop operation.

Motivated by the asymmetric dynamics of SMA actuation, this work proposes an asymmetric reset strategy designed to mitigate integral accumulation effects generated during passive recovery phases. The proposed controller introduces partial reset actions over the integral component of a PID controller, reducing accumulated error propagation while preserving tracking performance during actively controlled heating intervals. Closed-loop dynamics are derived using a phenomenological SMA model, and boundedness properties are analyzed through Lyapunov methods. Experimental validation is conducted using a biomimetic elbow actuation platform driven by SMA actuators under different operating conditions.

The remainder of the paper is organized as follows. Section 2 introduces SMA actuator characteristics and the phenomenological model. Section 3 presents the proposed reset control strategy and stability analysis. Section 4 describes the experimental setup and evaluation metrics. Finally, Section 5 presents experimental results, followed by conclusions in Section 6.

2. SMA Actuator

Shape Memory Alloys (SMAs) are smart materials capable of modifying their internal microstructure in response to temperature variations. When heated, the material recovers a previously imposed deformation, producing the Shape Memory Effect (SME). During this shape change, it can exert very high forces. Figure 1a depicts the SMA actuator employed in this work (NexmetalCorp (2026)), which consists of a Nitinol wire that contracts upon heating. The wire is introduced into a PTFE tube for electrical insulation and then into a Bowden cable to allow movement transmission.

The SME is produced by a reversible phase transformation between two crystallographic structures: martensite and austenite. Figure 1b illustrates the Stress–Strain–Temperature relationship of an SMA actuator during an actuation cycle. The austenitic phase appears at higher temperatures ($T > A_f$) and presents a more symmetric atomic arrangement. When the temperature decreases ($T < M_f$), the austenite transforms into twinned martensite, and when the material is deformed, detwinned martensite is produced. When the detwinned martensite is heated, it transforms back into austenite, recovering the previously applied strain and stress and returning to the material's original shape. During this actuation cycle, the material generates significant mechanical force, making SMA actuators especially suitable for applications requiring high force-to-weight ratios.

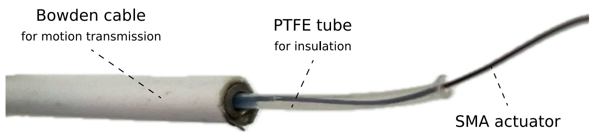

(a) Actuator integration

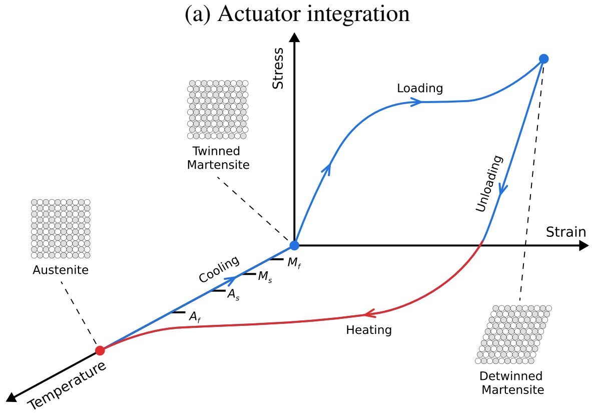

(b) Phase transformation curves

Figura 1: SMA actuator used in this work.

Heating can be achieved rapidly through the Joule effect by controlling the electrical excitation supplied to the actuator. However, the reverse transformation occurs through passive cooling, which is inherently slower because the material must dissipate heat before returning to the martensitic phase. Consequently, SMA actuators typically exhibit slow actuation dynamics dominated by the recovery process.

This operating principle introduces an intrinsic asymmetry between activation and recovery phases. This asymmetry represents a major challenge in SMA control systems, since tracking errors accumulated during recovery may affect subsequent actuation cycles. Therefore, SMA actuators require dedicated control strategies capable of accounting for these asymmetric dynamics in order to maximize tracking performance.

2.1. Phenomenological model

Although SMA materials exhibit highly nonlinear behavior including hysteresis, phase transition dynamics, and temperature-dependent properties, a phenomenological model is adopted to enable tractable stability analysis. Rather than describing the internal thermomechanical mechanisms, the model captures the dominant observable actuator dynamics. The SMA actuator is approximated as a slow first-order system, according to Equation (1), because its input–output behavior is largely governed by thermal dynamics, which introduce a dominant slow time constant in the actuation process. While simplified, this approximation captures the main response characteristics relevant for controller design and stability analysis, allowing the effect of the proposed reset strategy to be studied without introducing unnecessary thermomechanical complexity.

$$\tau\dot{x}(t) + x(t) = Ku(t) + d(t) \tag{1}$$

where $x(t)$ denotes the actuator displacement, $u(t)$ represents the control input associated with electrical excitation, K is the actuator gain, τ represents the dominant time constant, and $d(t)$ groups unmodeled dynamics and external perturbations. Despite its simplicity, this representation captures the slow response characteristic of SMA actuation and provides a suitable framework for closed-loop stability analysis.

3. Reset Controller

The control problem of Shape Memory Alloy (SMA) actuators presents an inherent asymmetry: the heating phase can be actively controlled through electrical excitation, whereas the recovery phase occurs naturally during cooling and cannot be directly actuated. Due to the slow rate of passive cooling, the actual position of the actuator remains above the reference, resulting in a negative error that saturates the integral toward negative values. Consequently, tracking errors accumulated during the passive recovery stage may persist and negatively influence the performance of subsequent actuation cycles.

To mitigate this effect, a reset control strategy is proposed. Reset control systems extend conventional linear controllers by introducing state discontinuities under predefined conditions, providing additional flexibility to improve transient performance and reduce accumulated errors Banos and Barreiro (2012). Unlike classical controllers, reset mechanisms allow selective state modifications while preserving the continuous dynamics during normal operation.

The controller dynamics are defined as a classical PID structure:

$$u(t) = K_p e(t) + K_i x_I(t) + K_d x_D(t) \tag{2}$$

where $e(t)$ denotes the tracking error, $x_I(t)$ represents the integral state, and $x_D(t)$ corresponds to the derivative contribution.

To improve robustness against measurement noise, the derivative component is filtered through a first-order dynamics:

$$\tau_D \dot{x_D}(t) + x_D(t) = \dot{e}(t) \tag{3}$$

The main characteristic of reset control lies in the discontinuous modification of selected controller states when predefined conditions are satisfied. In this work, only the integral component is reset, preventing error accumulation during the uncontrolled recovery phase and reducing its influence on subsequent operating cycles. In this work, the reset is applied when the error is below a certain negative value and when the position gradient is negative, meaning that the actuator is in recovery phase.

The reset law is defined as:

$$\begin{cases} \dot{x}_I(t) = e(t) & \text{when } e \geq \delta \\ x_I(t^+) = \gamma x_I(t) & \text{when } e(t) < \delta \text{ and } \nabla x(t) \leq 0 \end{cases} \tag{4}$$

where $\gamma \in (0, 1)$ determines the reset intensity and $\delta \in \mathbb{R}^-$ defines the reset band in which the reset event takes place. The parameter γ allows partial reset actions, preserving part of the accumulated integral contribution while introducing a dissipative mechanism that limits excessive error propagation.

3.1. System dynamics

The SMA actuator displacement can be expressed from the reference and tracking error relation as:

$$\dot{x} = \dot{r} - \dot{e} \tag{5}$$

Substituting Equation (2) and Equation (5) into the phenomenological model given in Equation (1), the closed-loop dynamics become:

$$\tau(\dot{r} - \dot{e}) + (r - e) = KK_p e + KK_i x_I + KK_d x_D + d \tag{6}$$

By expanding the terms and introducing suitable coefficient definitions, the closed-loop error dynamics can be written as:where the coefficients are defined as:

$$\dot{e} = -ae - bx_I - cx_D + \dot{r} + \frac{r}{\tau} + \Delta \tag{7}$$

where the coefficients are defined as:

$$\begin{cases} a = \frac{KK_p+1}{\tau} \\ b = \frac{KK_i}{\tau} \\ c = \frac{KK_d}{\tau} \\ \Delta(t) = -\frac{d(t)}{\tau} \end{cases} \tag{8}$$

This formulation isolates the tracking error dynamics and will be used in the subsequent stability analysis.

3.2. Lyapunov stability

To study the stability properties of the proposed reset controller, the following Lyapunov candidate function is considered, which captures the energy associated with the tracking error, integral state, and derivative state:

$$V = \frac{1}{2}e^2 + \frac{\alpha}{2}x_I^2 + \frac{\beta}{2}x_D^2 \tag{9}$$

For the continuous flow dynamics, the time derivative of the Lyapunov function is:

$$\dot{V} = e\dot{e} + \alpha x_I \dot{x}_I + \beta x_D \dot{x}_D \tag{10}$$

Substituting Equation (3) and Equation (7) into Equation (10), the time derivative of the Lyapunov function becomes:

$$\begin{aligned}\dot{V} &= e(-ae - bx_I - cx_D + \dot{r} + \frac{r}{\tau} + \Delta) + \alpha x_I e \\ &+ \frac{\beta}{\tau_D}x_D(-ae - bx_I - cx_D + \dot{r} + \frac{r}{\tau} + \Delta) - x_D)\end{aligned} \tag{11}$$

Expanding the terms yields:

$$\begin{aligned}\dot{V} &= -ae^2 - bex_I - cex_D + e\dot{r} + \frac{r}{\tau}e + e\Delta + \alpha x_I e \\ &- \frac{\beta a}{\tau_D}ex_D - \frac{\beta b}{\tau_D}x_I x_D - \frac{\beta c}{\tau_D}x_D^2 + \frac{\beta}{\tau_D}x_D\dot{r} \\ &+ \frac{\beta}{\tau\tau_D}rx_D + \frac{\beta}{\tau_D}x_D\Delta - \frac{\beta}{\tau_D}x_D^2\end{aligned} \tag{12}$$

And finally applying Young's inequalities to bound the cross-product terms and grouping coefficients leads to the uniform ultimate boundedness:

$$\dot{V} \leq -k_P e^2 - k_D x_D^2 + k_I x_I^2 + k_r r^2 + k_{\dot{r}}\dot{r}^2 + k_\Delta \Delta^2 \tag{13}$$

Equation (13) shows that the error and derivative dynamics contribute dissipative terms, whereas the integral component introduces energy into the system. Therefore, under bounded reference trajectories and disturbances, the closed-loop energy remains limited, ensuring bounded-state behavior during continuous evolution. While the trajectory error converges to zero for step reference signals, for variable references, such as sinusoidal signals, the error remains bounded.

During reset events, only the integral component is modified according to Equation (4). Therefore, the variation of the Lyapunov candidate function across reset instants is:

$$V^+ - V^- = \frac{\alpha}{2}(\gamma^2 - 1)x_I^2 \tag{14}$$

Since $\gamma^2 - 1 \leq 0$, it follows that:

$$V^+ - V^- \leq 0 \tag{15}$$

This result shows that reset events introduce an inherently dissipative mechanism by removing part of the accumulated integral energy. Consequently, the reset action counteracts integral error growth and improves the boundedness properties of the closed-loop system.

4. Experimental Setup

4.1. Test Bench

Experimental validation was conducted using a test bench designed to emulate the motion of a human elbow joint. The platform consists of anatomically inspired arm bone models acting as structural fixation components, where the conventional biceps muscle is replaced by the proposed SMA actuator.

Figure 2 shows the experimental setup employed in this work. The SMA actuator generates linear contraction during heating, which is then converted into rotational motion of the forearm structure through a tendon transmission mechanism based on Kevlar wire, reproducing the flexion movement of the elbow joint.

Actuator position is measured using a Hall-effect sensor (MouserElectronics (2026)) coupled to a multipole strip magnet attached to the moving SMA mechanism. As the SMA wire contracts, the relative displacement between the magnet and the sensor changes, allowing continuous position estimation for feedback control purposes. The complete platform enables experimental evaluation of SMA actuation under biomechanically representative operating conditions while providing repeatable measurements for controller validation.

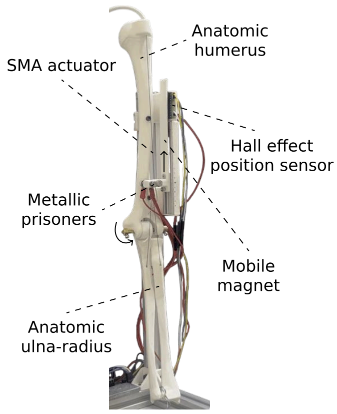

Figura 2: Biomimetic elbow test bench driven by SMA.

4.2. Data acquisition

The proposed Reset controller is compared to a conventional PID controller using sinusoidal signals under three actuation amplitudes (10, 20, and 30 mm) and three oscillation periods (15, 30, and 60 s). Each operating condition was executed for six consecutive actuation cycles using both controllers. This experimental protocol allows evaluating controller performance under different operating speeds and motion amplitudes while capturing the influence of error accumulation across repeated SMA activation cycles. Table 1 shows the designated parameters for each controller, obtained experimentally to fit the experiments.

The data acquisition and control execution were performed using a Raspberry Pi embedded platform. The Raspberry Pi continuously acquires sensor measurements, computes the control law, and generates the PWM control signal employed to drive the SMA actuator, using a sampling period of 10 ms. Since SMA actuators require current amplification beyond the capabilities of the embedded controller, the PWM signal is transmitted to a dedicated power stage responsible for supplying the electrical current required for Joule heating.

Tabla 1: PID and Reset PID parameters

	K_p	K_d	K_i	δ (mm)	γ
PID	80	10	30	-1.0	1.0
RPID	80	10	30	-1.0	0.3

4.3. Metrics

Three quantitative performance metrics were employed to compare controller behavior: Root Mean Square Error, fit score and Integral Absolute Control demand. The Root Mean Square Error (RMSE) is used to evaluate global trajectory tracking performance:

$$\mathrm{RMSE} = \sqrt{\frac{1}{N}\sum_{i=1}^{N}(r_i - x_i)^2} \quad (16)$$

where r_i denotes the reference position and x_i represents the measured actuator position for each test sample i.

Additionally, to provide a normalized performance indicator independent of trajectory amplitude, the fit score ϕ is introduced:

$$\phi = 1 - \frac{\mathrm{RMSE}}{\mathrm{RMS}(r)} \quad (17)$$

where $\mathrm{RMS}(r)$ corresponds to the root mean square value of the reference trajectory.

Since SMA recovery dynamics occur through passive cooling and cannot be directly actuated, the heating-phase tracking metric are isolated to study the active performance of both controllers. The heating Root Mean Square Error (RMSE_{heat}) and the heating fit score (ϕ_{heat}) are computed exclusively during intervals in which the control signal is positive, obtaining tracking performance during actively controlled actuation.

Finally, the Integral Absolute Control demand (IAC) was employed to quantify accumulated controller action:

$$\mathrm{IAC} = \int_0^{TN_c} |u(t)|dt \quad (18)$$

where T is the signal period, N_c is the number of cycles and $u(t)$ corresponds to the unsaturated controller output, before the PWM generation. This metric evaluates accumulated control demand and provides an indirect indicator of integral accumulation effects.

5. Results

The proposed Reset Controller was experimentally compared against a conventional PID controller under the operating conditions defined previously in Section 4.2. Figure 3 shows representative experimental responses obtained for both controllers, including actuator position tracking and controller output evolution.

Figure 3a shows that both controllers achieve comparable global tracking performance. Due to the dominant influence of passive cooling dynamics in SMA actuators, overall trajectory errors remain similar between both approaches during the recovery phase. However, differences become evident after the first cycle, where accumulated error in the PID controller delays actuator heating and introduces tracking deviations in the actuator position. The reset strategy reduces accumulated integral action generated by recovery phase errors, allowing the controller to initiate actuator heating as soon as the tracking error becomes positive again. As a consequence, the Reset Controller exhibits improved reference tracking during heating intervals while preserving stable closed-loop operation over consecutive actuation cycles.

Figure 3b illustrates the evolution of the controller signal for both control strategies. The conventional PID controller tends to accumulate larger control demands during repeated operation cycles, particularly when recovery dynamics introduce persistent tracking deviations. In contrast, the Reset Controller limits this accumulation by partially resetting the integral contribution under predefined operating conditions, causing the control signal to be primarily dominated by the proportional term, which does not introduce delays.

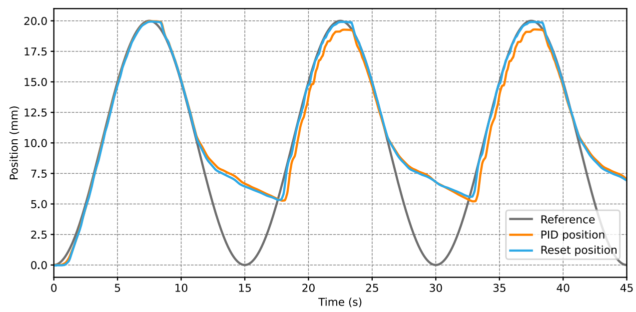

(a) Measured position

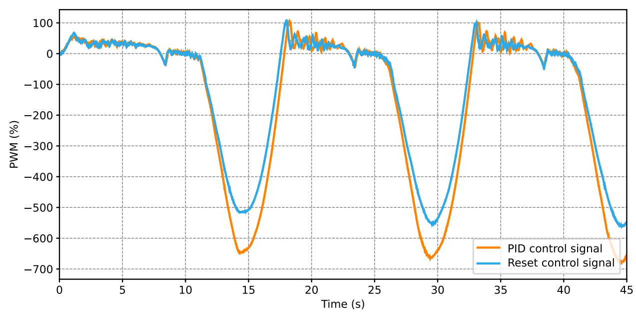

(b) Unsaturated control signal

Figura 3: Experimental comparison between PID and Reset PID controllers.

Table 2 shows the quantitative data obtained for the comparison and validation of the Reset Controller. In general, for slower actuation conditions, differences between controllers become less pronounced. Since slower trajectories naturally reduce error accumulation between consecutive activation cycles, the benefit introduced by the reset mechanism decreases as the operating period increases.

Tabla 2: PID and Reset PID quantitative performance comparison.

Controller	T (s)	RMSE (mm)	$RMSE_{heat}$ (mm)	ϕ_{heat}	IAC $\times 10^6$(% · s)
PID	15	3,01 ± 0,38	1,06 ± 0,02	0,92 ± 0,04	7,85 ± 1,36
	30	2,02 ± 0,30	0,69 ± 0,02	0,94 ± 0,03	7,47 ± 1,56
	60	0,63 ± 0,30	0,34 ± 0,01	0,97 ± 0,01	1,97 ± 1,40
RPID	15	3,04 ± 0,45	0,33 ± 0,04	0,97 ± 0,01	5,47 ± 1,51
	30	1,66 ± 0,65	0,21 ± 0,01	0,98 ± 0,01	3,71 ± 2,23
	60	0,72 ± 0,27	0,18 ± 0,07	0,98 ± 0,01	1,49 ± 0,72

The total RMSE is very similar for both controllers, since it also includes the tracking error corresponding to the recovery phase. However, performance metrics associated with the actively controlled actuation phase, such as $RMSE_{heat}$, show an improvement in trajectory tracking performance when using the Reset Controller, resulting in more accurate actuator motion. The fit score ϕ_{heat} also improves for the Reset Controller. It also can be observed that the fit score decreases with increasing actuation frequency for the PID controller, whereas the Reset Controller maintains consistently higher values across all tested frequencies.

Additionally, the Integral Absolute Control demand is reduced when employing the reset strategy, indicating that the controller achieves comparable global performance and improved activation tracking performance while requiring less accumulated corrective action. This behavior is consistent with the theoretical analysis presented in Section 3.2, where reset events introduce a dissipative mechanism that limits excessive integral accumulation.

Overall, the experimental observations support the proposed hypothesis that phase-dependent reset actions mitigate integral accumulation effects associated with SMA asymmetric recovery dynamics while preserving stable tracking performance.

6. Conclusions

This work presented an asymmetric reset control strategy for SMA actuators that reduces error propagation between consecutive activation cycles. Experimental validation demonstrates that the proposed controller preserves comparable global tracking performance while improving tracking accuracy during actively controlled heating intervals. The reset improvement becomes more relevant under faster operating conditions, where thermal dynamics introduce stronger error accumulation.

The proposed strategy is straightforward to implement, preserves closed-loop boundedness properties, and improves actuator responsiveness while enhancing tracking performance. These results support reset control as a promising approach for SMA actuation systems exhibiting asymmetric thermal dynamics.

Referencias

Al Janaideh, M., Al Saaideh, M., Tan, X., April 2023. The prandtl-ishlinskii hysteresis model: Fundamentals of the model and its inverse compensator [lecture notes]. IEEE Control Systems 43 (2), 66–84.
URL: `https://doi.org/10.1109/MCS.2023.3234381`
DOI: `10.1109/mcs.2023.3234381`

Banos, A., Barreiro, A., 2012. Reset Control Systems. Springer London.
URL: `https://doi.org/10.1007/978-1-4471-2250-0`
DOI: `10.1007/978-1-4471-2250-0`

Copaci, D.-S., Blanco, D., Martin-Clemente, A., Moreno, L., January 2020. Flexible shape memory alloy actuators for soft robotics: Modelling and control. International Journal of Advanced Robotic Systems 17 (1).
URL: `https://doi.org/10.1177/1729881419886747`
DOI: `10.1177/1729881419886747`

Costanza, G., Tata, M. E., April 2020. Shape memory alloys for aerospace, recent developments, and new applications: A short review. Materials 13 (8), 1856.
URL: `https://doi.org/10.3390/ma13081856`
DOI: `10.3390/ma13081856`

Jadhav, M. R., Singh, S., John, P., Bhargaw, H. N., Rajak, D. K., March 2025. Advancements and recent trends in shape memory alloy actuators: position control and emerging applications. International Journal of Dynamics and Control 13 (3).
URL: `https://doi.org/10.1007/s40435-025-01615-8`
DOI: `10.1007/s40435-025-01615-8`

Karbasizadeh, N., HosseinNia, S. H., September 2022. Continuous reset element: Transient and steady-state analysis for precision motion systems. Control Engineering Practice 126, 105232.
URL: `https://doi.org/10.1016/j.conengprac.2022.105232`
DOI: `10.1016/j.conengprac.2022.105232`

Mandolino, M. A., Scholtes, D., Ferrante, F., Rizzello, G., October 2023. A physics-based hybrid dynamical model of hysteresis in polycrystalline shape memory alloy wire transducers. IEEE/ASME Transactions on Mechatronics 28 (5), 2529–2540.
URL: `https://doi.org/10.1109/TMECH.2023.3253250`
DOI: `10.1109/tmech.2023.3253250`

MouserElectronics, 2026. Nse-5310-assu ams osram — mouser spain. `https://www.mouser.es/ProductDetail/ams-OSRAM/NSE-5310-ASSU?qs=jMXWnm70%252BC%252B0DhXBWRQPUA%3D%3D`, accessed: 21 January 2026.

NexmetalCorp, 2026. Nitinol linear actuator (2 way) shape memory alloy wire – nexmetal corporation. `https://nexmetal.com/products/nitinol-linear-actuator?variant=39514873987114`, accessed: 25 May 2026.

Patterson, Z. J., Sabelhaus, A. P., Majidi, C., April 2022. Robust control of a multi-axis shape memory alloy-driven soft manipulator. IEEE Robotics and Automation Letters 7 (2), 2210–2217.
URL: `https://doi.org/10.1109/LRA.2022.3143256`
DOI: `10.1109/lra.2022.3143256`

Shi, E., Zhong, X., Wang, T., Li, X., Bu, C., Zhao, X., January 2024. Adaptive control for shape memory alloy actuated systems with applications to human-robot interaction. Frontiers in Neuroscience 18.
URL: `https://doi.org/10.3389/fnins.2024.1337580`
DOI: `10.3389/fnins.2024.1337580`

Utter, B., October 2019. Enhancing the actuation frequency of shape memory alloy wire by vibration-enhanced cooling. Journal of Intelligent Material Systems and Structures 30 (20), 3177–3189.
URL: `https://doi.org/10.1177/1045389X19880015`
DOI: `10.1177/1045389x19880015`

Zhang, X., HosseinNia, S. H., November 2025. Enhancing reset control phase with lead shaping filters: Applications to precision motion systems. Control Engineering Practice 164, 106482.
URL: `https://doi.org/10.1016/j.conengprac.2025.106482`
DOI: `10.1016/j.conengprac.2025.106482`